High-performance field emission device utilizing vertically aligned carbon nanotubes-based pillar architectures

Bipin Kumar Gupta, Garima Kedawat, Amit Kumar Gangwar, Kanika Nagpal, Pradeep Kumar Kashyap, Shubhda Srivastava, Satbir Singh, Pawan Kumar, Sachin R. Suryawanshi, Deok Min Seo, Prashant Tripathi, Mahendra A. More, O. N. Srivastava, Myung Gwan Hahm, and Dattatray J. Late

Citation: AIP Advances **8**, 015117 (2018); doi: 10.1063/1.5004769

View online: https://doi.org/10.1063/1.5004769

View Table of Contents: http://aip.scitation.org/toc/adv/8/1

Published by the American Institute of Physics

High-performance field emission device utilizing vertically aligned carbon nanotubes-based pillar architectures

Bipin Kumar Gupta,[1,a] Garima Kedawat,[1] Amit Kumar Gangwar,[1,2] Kanika Nagpal,[1] Pradeep Kumar Kashyap,[1,2] Shubhda Srivastava,[1,2] Satbir Singh,[1,2] Pawan Kumar,[1,2] Sachin R. Suryawanshi,[3] Deok Min Seo,[4] Prashant Tripathi,[5] Mahendra A. More,[3] O. N. Srivastava,[5] Myung Gwan Hahm,[4,b] and Dattatray J. Late[6,c]

[1]*CSIR- National Physical Laboratory, Dr K S Krishnan Road, New Delhi 110012, India*
[2]*Academy of Scientific and Innovative Research (AcSIR), CSIR-National Physical Laboratory Campus, Dr K S Krishnan Road, New Delhi 110012, India*
[3]*Centre for Advanced Studies in Materials Science and Condensed Matter Physics, Department of Physics, Savitribai Phule Pune University, Pune 411007, India*
[4]*Department of Materials Science and Engineering, Inha University, 100 Inharo, Nam-Gu, Incheon 22212, Republic of Korea*
[5]*Nanoscience Centre, Department of Physics (Centre of Advanced Studies), Institute of Science, Banaras Hindu University, Varanasi 221005, India*
[6]*CSIR - National Chemical Laboratory, Dr. Homi Bhabha Road, Pashan, Pune 411008, India*

(Received 15 September 2017; accepted 1 January 2018; published online 12 January 2018)

The vertical aligned carbon nanotubes (CNTs)-based pillar architectures were created on laminated silicon oxide/silicon (SiO_2/Si) wafer substrate at 775 °C by using water-assisted chemical vapor deposition under low pressure process condition. The lamination was carried out by aluminum (Al, 10.0 nm thickness) as a barrier layer and iron (Fe, 1.5 nm thickness) as a catalyst precursor layer sequentially on a silicon wafer substrate. Scanning electron microscope (SEM) images show that synthesized CNTs are vertically aligned and uniformly distributed with a high density. The CNTs have approximately 2–30 walls with an inner diameter of 3–8 nm. Raman spectrum analysis shows G-band at 1580 cm^{-1} and D-band at 1340 cm^{-1}. The G-band is higher than D-band, which indicates that CNTs are highly graphitized. The field emission analysis of the CNTs revealed high field emission current density (4mA/cm^2 at 1.2V/μm), low turn-on field (0.6 V/μm) and field enhancement factor (6917) with better stability and longer lifetime. Emitter morphology resulting in improved promising field emission performances, which is a crucial factor for the fabrication of pillared shaped vertical aligned CNTs bundles as practical electron sources.
https://doi.org/10.1063/1.5004769

I. INTRODUCTION

New exotic nanoforms of carbon such as graphene, carbon nanotubes (CNTs), carbon nanocups have been designated as potential contenders for variety of structure in future generations wide range of applications such as flat panel displays, X-ray and advanced electronic devices.[1–3] Conductivity, resistance of emitter/substrate interfaces, surface work function of material and emitter tip quality are some of the important factors which determine the efficiency of field-emission.[2,4] For field emission display applications, it is necessary to grow vertically aligned carbon nanotube (CNT) arrays on a

[a]Authors to whom correspondence should be addressed. Electronic mail: bipinbhu@yahoo.com.
[b]mghahm@inha.ac.kr
[c]dj.late@ncl.res.in

large scale with suitable emitter density and high aspect ratio.[2,4,5] Among different structure of CNTs, pillar-shaped vertically aligned CNTs exhibit several supportive properties such as an electron source emitter, high aspect ratio, radius of curvature in nano regime, low stiffness, excellent chemical inertness, better thermal stability, and good mechanical strength.[5] Vertically aligned CNTs also known as a CNT forest, are a porous material that is well known for its exceptional optical absorbance property. The growth of periodic arrays of pillar-shaped vertically aligned CNTs on a large area having same structure, dimension, high packing density, and ordered arrangement are essential criteria for practical applications of field emission sources.[6] The improvement of the field emission current density and reduction of the emission turn-on voltage are the main goals in the field emission applications. CNTs have an good advantage in strong electric fields that on the emitting surface, any significant shape changes doesn't occur, which in particular could lead to unstable operation of metal nano tip-based field emitting devices.[7] The average inter-nanotube spacing has been one of the most common practical solutions to maximize the electron field emission yield.[8] The pillar-shaped vertically aligned CNTs can be significantly affected due to the mutual field screening effect caused by the proximity of neighboring tubes in the array.[7] This effect determines the optimal inter-tube distance providing the maximum emission current density for the array. The emission characteristic from these arrays is the natural statistical spread in geometry in individual nanotubes. The higher emission current is due to the most protruded nanotubes having maximum value of the aspect ratio of nanotubes.

The various nanofabrication techniques and approaches have been successfully used to synthesize carbon nanotube-based functional nanoscale assemblies and architectures. In recent years, chemical vapor deposition (CVD) technique has been widely introduced to produce vertically aligned, periodic, similar alignment, orientation, and lengths of nanostructure arrays having high aspect ratio.[9–11] Their symmetry is related to the orientation of the hexagonal lattice with respect to the axis of the tube. Although many researchers have worked on different catalysts to synthesize pillar-shaped vertically aligned CNTs but still there is a lot of permutation and combination required to prepare a low cost catalyst which can enhance the growth rate, purity as well as crystalline structure of the CNTs suitable for different applications.

In this article, pillar-shaped vertically aligned CNT architectures have been synthesized by using a single-step water-assisted CVD process that shows promising field-emission characteristics. This synthesis process usually involves different catalysts, barrier layers, carbon sources, and operation parameters, resulting in products with different morphologies and qualities. In water-assisted CVD synthesis process, the substrate SiO_2/Si wafer supports the growth of CNTs where aluminium (Al) as a barrier layer and iron (Fe) as a catalyst for growth of CNTs. We investigated the electron emission characteristics from pillar-shaped vertically aligned CNTs architectures using a parallel plate configuration for macroscopic emission characteristics and a 1 mm tungsten anode for microscopic emission measurements from individual nanotube. The resulting macroscopic pillar-shaped vertically aligned bundles allows the emission current to be shared among many CNTs, providing low threshold fields and hence, increases lifetime and durability. The structure of as-synthesized vertically aligned CNTs-based pillar architectures are evaluated using scanning electron microscopy (SEM), transmission electron microscopy (TEM), and Raman spectroscopy.

II. EXPERIMENTAL

A. Synthesis of pillar-shaped vertically aligned carbon nanotubes architectures

The pillar-shaped vertically aligned CNTs were synthesized by using a water-assisted CVD technique. Initially, SiO_2/Si wafer (011) was cleaned ultrasonically and dried at room temperature. Electron-beam evaporation was employed to deposit Al (10.0 nm) as a barrier layer and Fe (1.5 nm) as a catalyst sequentially on a silicon wafer substrate with SiO_2 of 500 nm thickness with shadow mask to create square patterns. The silicon wafer was then cut into small pieces (0.5 cm × 0.5 cm) and put into a quartz tube. The quartz tube containing the substrate was positioned in the tube furnace under the protection of Ar- balanced H_2 mixture gas (15 vol% H_2) and the temperature was heated upto 775 °C within 15min. Then, ethylene gas (100 sccm) as a carbon source and water vapor was

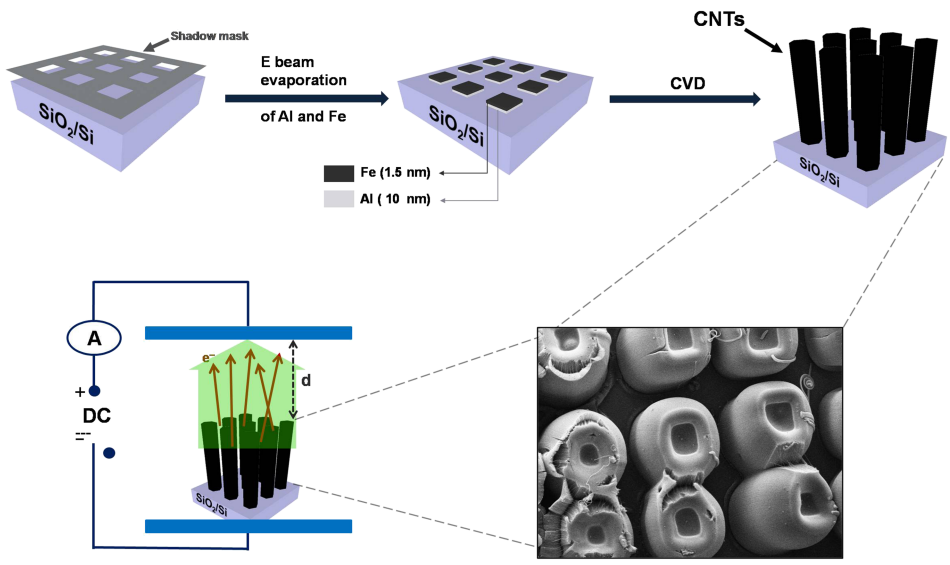

FIG. 1. Schematic demonstration of the fabrication process along with their SEM image of the vertically aligned carbon nanotubes-based pillars and method for the field emission measurement of pillar-shaped aligned carbon nanotubes architectures.

introduced into the quartz tube to start the synthesis of pillar-shaped vertically aligned CNTs. The CNTs growth was carried out at 2.42 Torr for a further 15 min. The flow of ethylene was stopped after15 min of the CNTs growth, and then finally, the furnace is cooled down to room temperature. The dimension of the sample area is 0.5∗0.5 cm^2 and distance of anode to cathode is 1 mm. The schematic diagram and their SEM image of the fabrication of pillar-shaped vertically aligned CNTs architectures is shown in Fig. 1. The simple field emission device utilizing pillar-shaped vertically aligned CNTs was fabricated as shown in schematic drawing (Figure 1).

B. Characterization

After removing the samples from the quartz tube, morphological analyses were performed using high-resolution SEM (HRSEM; EVO-MA 10 VPSEM) operated at 5 kV to determine the height and morphology of as-synthesized architectures, precisely. The height was measured at several places and the mean height was estimated. The internal structure of the as-grown carbon nanostructures was examined by removing the CNTs from the substrates, dispersed in methanol, drop-casted on a copper grid, and observed the grids by high-resolution TEM (HRTEM; Technai G20-twin, 300 kv with super twin lenses having point and line resolution of 0.144 nm and 0.232 nm, respectively). Spectroscopic analyses were carried out using a micro-Raman spectrometer (Renishaw in Via Co., England) with an Ar-ion laser a wavelength of 514 nm as the excitation light source. The spot size was 15 μm and laser power was around 6 mW. A parallel-plate configuration was used for field-emission measurements of as-grown samples in a high vacuum chamber (base pressure of 10^{-7} Torr), with a sample acting as the cathode and a phosphor-coated indium tin oxide (ITO) glass electrode acting as the anode for the visualization of field emission sites distribution. The distance between the cathode and the anode (100μm) was adjusted using micrometer screw gauge arrangement. The field emission current was measured at different voltages using an automatically controlled Keithley 2001 electrometer and power supply (Fug Power HCN 700–3500) with pico-ampere sensitivity. All measurements were performed at room temperature.

III. RESULTS AND DISCUSSION

The side- and top-view of well-aligned and three-dimensional architectures of pillar-shaped vertically aligned CNTs is shown in Fig. 2(a) and 2(b). The magnified view of Fig. 2(b) is given in Fig. 2(c) and 2(d). The surfaces of CNTs grown at 2.42 torr were smoother. It revealed that

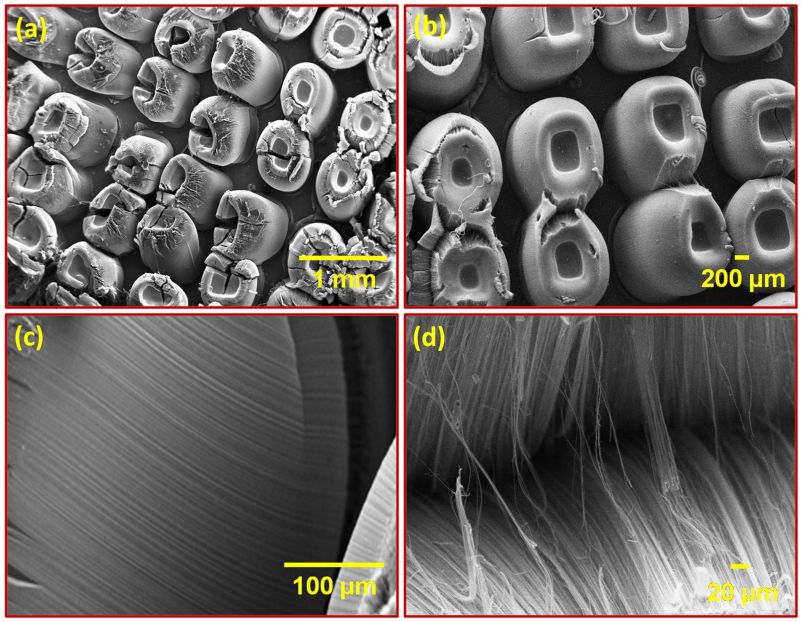

FIG. 2. (a) Side and (b) top view of pillar-shaped vertically aligned and three-dimensional CNTs, (c) and (d) magnified view of fig. 2b.

the vertically aligned, uniformly distributed and relatively high density CNTs have the heights up to several millimeters. The CNTs consist of 2–30 walls with an inner and outer diameter of 3–8 nm and 12-16 nm, respectively. In the orientation of CNTs, the outer wall of each nanotube interacts with the outer walls of neighboring nanotubes due to nm, vander Waals interaction, which results to form large bundles with sufficient rigidity to keep the growth direction.[12] It means that the density of CNTs approaches the aligned growth. This can be clearly seen in Fig. 2(a) and 2(b). The similar growth process of pillar-shaped vertically aligned CNTs with same efficiency is also shown in Fig. S1 (see supplementary material).

A typical HRTEM image of vertically aligned CNTs-based pillar architectures is given in Fig. 3. It displays the structures of as-synthesized CNTs. It is clearly seen that the number of walls of tubes are 2–30 and the distribution of diameters is 3-6 nm. As a result, good efficiency in the growth of pillar-shaped vertically aligned CNTs grown was observed. To investigate the vibrational properties and electronic structures of CNT, particularly, for the characterization of CNTs with respect to their

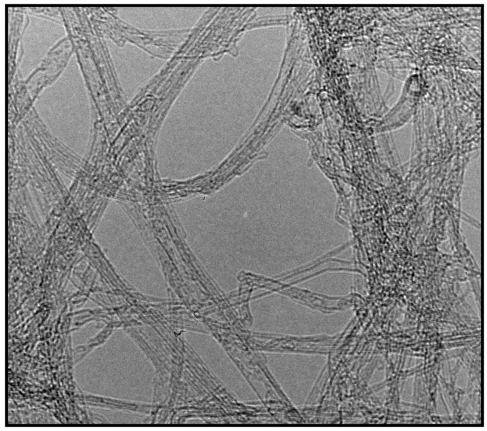

FIG. 3. HRTEM image of as-grown CNTs.

diameters and quality of the sample properties, Raman spectroscopy has been used. The crystalline quality can be determined using ratio of intensities of D-band and G-band peaks. The Raman spectrum of as-grown vertically aligned CNTs is shown in Fig. S2 (see supplementary material). In the spectrum recorded from as-grown CNTs, D-band and G-band appears at 1340 cm^{-1} and 1580 cm^{-1}, respectively. The peak intensity of G-band is higher than as that of the D-band, which indicates that CNTs have highly graphitic nature. There is also another peak found at 2670 cm^{-1}, which may be due to the amorphous carbon.[13,14]

The vertically aligned CNTs-based pillar architectures have tens of thousands of atomically sharp tips that enhance the field emission properties. Fig. 4 shows the field emission behavior of pure pillar-shaped vertically aligned CNTs. Particularly for the case of field emitters on two dimensional thin film substrates, the modified Fowler-Nordehim equation for current density (J) and the applied electric field E is as follows,[15–17]

$$J = \lambda_M \, a \, (\beta^2 E^2/\phi) \exp(-b\phi^{3/2} \nu_F / \beta E)$$

Where, λ_M is macroscopic pre-exponential correction factor, a = (1.54 x 10^{-6}AeV V^{-2}) and b = (6.83 $VeV^{-3/2}$ nm^{-1}) are constants, ϕ is the work function, β is field enhancement factor and ν_F (correction factor) is a particular value of the principal Schottky-Nordheim barrier function v.

The plot of the field emission current density (J) versus applied electric field (E) for vertically aligned CNTs-based pillar architectures is exhibited in Fig. 4(a). In general, the field emission characteristics are closely related with emitter's dimensions, high aspect ratio (1:10 ~ 15) of pillar-shaped vertically aligned CNTs. i.e. The turn-on voltage and threshold field, defined as, the field required for drawing emission current densities of ~1 μA/$cm^2$and ~10 μA/$cm^2$are found to be 0.6 V/μm and ~0.7 V/μm, respectively for the pillar architectures. The emission current is dramatically increased and the emission current density (~4 mA/cm^2) is drawn at an applied field (~1.2 V/μm) as the applied

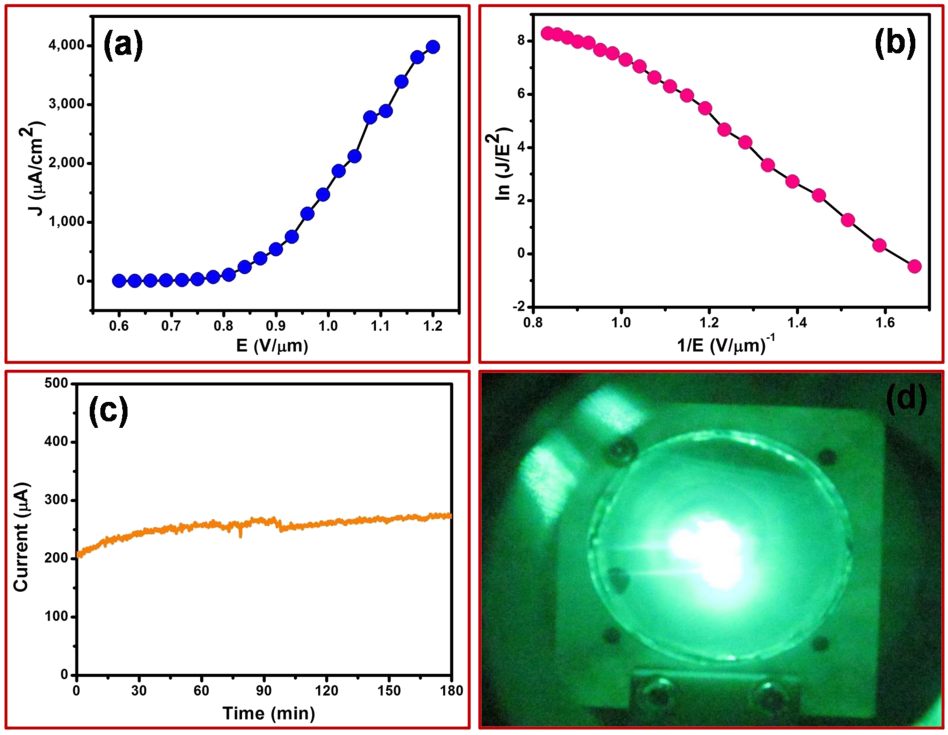

FIG. 4. (a) Plot of emission current density as a function of applied electrical field,(b) F-N plot indicating nonlinear characteristics of emission current from the pillar-shaped vertically aligned CNTs emitter, (c) plot of current vs time showing long term field emission current stability and (d) illuminating image of field emission taken during the long-term stability study of the emitter.

voltage is increased. It was corresponded with Fowler-Nordehim theory. It is clearly seen that synergistic combination of high aspect ratio, atomically sharp diameter of emission tip (CNTs), uniform distribution of emission tips over the whole area of the specimen, and lower screening effect of vertically aligned CNTs give rise to observed superior values of turn-on and threshold field, and extraction of high emission current density at lower applied electric field. In present case of specially architecture pillar-shaped vertically aligned CNTs structure, the electric potential forms in the vicinity of the tip of each nanotubes is screened by neighbouring nanotubes via single pillars, so that the electric field strength depends notably on the density of nanotubes arrays in pillar structures. Similarly, the bunch of pillars also supposed the further reduced screening effect. This optimum arrangement of pillar structures leads to provide vertically aligned emitters having moderate number density and gives the weak influence of screening effect.

It can be noticed that burning problem in CNTs doesn't affected during the measurement process. It is well established that the wall of CNTs damage in term of split patch by patch and segment by segment. CNTs are damage following a string by string removing of the carbon atoms along the circumference of the graphitic layers.[18,19] To avoid such situation, geometrical architecture of nanotubes is very important. In our present case, vertically aligned carbon nanotubes-based pillar architectures are proposed, where the small damage in one or two string walls, doesn't make any significant difference in the results. In addition to the above, the field emission behaviour of same sample for different cycle runs (1st, 3rd, 5th and 10th cycles) are also examined, as shown in Fig. S3 (see supplementary material). It shows better emission uniformity and a good reproducibility of field emission behaviour during the different cycle run. Furthermore, the field emission characteristics of different as-synthesized samples of pillared shaped vertically aligned carbon nanotubes (sample 1, sample 2, sample 3 and sample 4) are also examined to explore reproducibility and the results are shown in Fig. S4 (see supplementary material). It can be noticed that all the samples show similar and consistent behaviour.

Fig. 4(b) showed the Fowler-Nordehim curve estimated by field emission properties recorded from vertically aligned CNTs field emitter. The calculated field enhancement factor is ~6917 from slope of the Fowler-Nordehim plotin the linear region. The Fowler-Nordehim curve for the vertically aligned CNTs-based pillar architectures field emitter shows linear characteristic. The trend of the curve indicates saturation at high electric fields. The enhancement of the electric field at the emitter can be determined by the field enhancement factor owing to atomically sharp tips with their nano-metric protrusions.[2] The calculated field enhancement factor of vertically aligned CNTs-based emission device from the slope of the Fowler-Nordehim plot is ~ 6917 by considering work function (ϕ) of the emitter ~5 eV for CNTs. Zanin et al. calculated theoretical geometrical enhancement factor β around 2000 on the basis of the ratio of height and radius of individual nanotubes.[20] In present case, the higher enhancement factor β is due to the special geometry of the vertical aligned CNTs providing enhancement in local electric field in pillar structure, as a result emission integrates multifold times due to several adjacent emitting tip rather than being from one isolated CNTs. The enhancement factor increases enormously as compared to the theoretical limits of vertical aligned CNTs.

The typical long persistent current stability (I-t) of a pillar-shaped vertically aligned CNTs field emitterat a pressure of ~1 x 10^{-8} mbar is shown in Fig. 4(c). To develop the emission characteristics of CNTs in field emission device applications, invariable emission current stability is indispensable for the production of field emission nano-electronic devices. Fig. 4(c) shows the field emission current stability outlines for vertically aligned CNTs-based pillar architectures at ~200 μA for a sampling interval of 10 m sec recorded up to 3 hours. The mean emission current was stable during the measurement. It substantiated that vertically aligned CNTs-based emission tips have no damaging effects and show their mechanical strength oppose to ion bombardment and field-induced stress. Fig. 4(d) shows the typical illuminating field emission image of the vertically aligned CNTs-based pillar architectures field emitter recorded at a current density of ~500 μA/cm^2.

IV. CONCLUSIONS

In conclusions, the water-assisted CVD was used to synthesize vertically aligned CNTs-based pillar architectures on laminated Si wafer substrate. The lamination was carried out at low pressure

process conditions and simultaneously heating it at 775 °C. The SEM micrograph shows a uniform growth of vertically aligned CNTs of diameter 3-8 nm. Raman spectra of CNTs sample shows that CNTs are highly graphitized. Field emission analysis of the as-grown the pillar-shaped vertical aligned CNTs shows good field emission properties with low turn-on field 0.6 V/μm, the high current density of 4mA/cm^2 at 1.2V/μm and the enhancement factor is 6917. The comparison of field emission characteristic of pillared shaped vertically aligned carbon nanotubes with recent published literature is also given in Table TS1 (see supplementary material).[21–25] Thus, the highly stable vertically aligned CNTs-based pillar architectures having low turn on field are showing great potential as an emerging electron emitter for futuristic nano-electronics and thin film-based display applications.

SUPPLEMENTARY MATERIAL

See supplementary materials for SEM image for top view of pillared shaped vertically aligned carbon nanotubes architectures, raman spectrum, field emission properties of same sample for different cycle runs, Field emission characteristics of different as-synthesized samples of pillared shaped vertically aligned carbon nanotubes and comparison of field emission characteristic of pillared shaped vertically aligned carbon nanotubes with recent published literature.

ACKNOWLEDGMENTS

The authors wish to thank Director, N.P.L. New Delhi, for his keen interest in the work. The authors express their thankfulness and appreciation to Prof. R. C. Budhani (former Director, NPL and professor at IIT Kanpur) for his constant support and encouragement during the work. P. K. Kashyap, S. Singh, P. Kumar, A. K. Gangwar gratefully acknowledged University Grant Commission (UGC) and Council of Scientific and Industrial Research (CSIR), Govt. of India for financial assistance to carry out this work. S. Srivastava gratefully acknowledges the financial support from Department of Science and Technology India under woman Scientist Scheme A. Mr. SachinSuryawanshi gratefully acknowledges the financial support from BARC, Mumbai, for the award of Senior Research. Fellowship under BARC-UoP memorandum. Prof. M. A. More would like to thank the BCUD, University of Pune for the financial support provided for the field emission work under CNQS-UPE-UGC program activity. Dr. D. J. Late thank to DST for Grant No. SR/S2/RJN-130/2012 and NCL-MLP project grant, DST-SERB Fast-track Young scientist project, BRNS Project34/14/20/2015; INUP IITB project sponsored by Deit Y, MCIT, Government of India. M.G.H. are grateful for the support of the National Research Foundation of Korea (NRF) grant funded by the Ministry of Education (NRF-2017R1D1A1B03030225).

[1] H. Chun, M. G. Hahm, Y. Homma, R. Meritz, K. Kuramochi, L. Menon, L. Ci, P. M. Ajayan, and Y. J. Jung, ACS Nano **3**, 1274–1278 (2009).
[2] B. K. Gupta, G. Kedawat, P. Kumar, S. Singh, S. R. Suryawanshi, N. Agrawal (Garg), G. Gupta, A. R. Kim, R. K. Gupta, M. A. More, D. J. Late, and M. G. Hahm, RSC Adv. **6**, 9932–9939 (2016).
[3] W. Wang, X. Qin, N. Xu, and Z. Li, J. Appl. Phys. **109**, 044304 (2011); C. S. Rout, P. D. Joshi, R. V. Kashid, D. S. Joag, M. A. More, A. J. Simbeck, M. Washington, S. j. K. Nayak, and D. J. Late, Nature Sci. Rep. **3**, 3282 (2013); B. A. Kakade, V. K. Pillai, D. J. Late, P. G. Chavan, F. J. Sheini, M. A. More, and D. S. Joag, Appl. Phy. Lett. **97**, 73102 (2010); A. K. Samantara, D. K. Mishra, S. R. Suryawanshi, M. A. More, R. Thapa, D. J. Late, B. Kumar Jena, and C. S. Rout, RSC Adv. **6**, 41887–41893 (2015); R. Khare, D. B. Shinde, S. Bansode, M. A. More, M. Majumder, V. K. Pillai, and D. J. Late, Appl. Phy. Lett. **2**, 23111 (2015).
[4] B. K. Gupta, D. Haranath, S. Chawla, H. Chander, V. N. Singh, and V. Shanker, Nanotechnol. **21**, 225709 (2010).
[5] H. J. Kim, J. H. Han, W. S. Yang, J. B. Yoo, C. Y. Park, I. T. Han, Y. J. Park, Y. W. Jin, J. E. Jung, N. S. Lee, and J. M. Kim, Mater. Sci. Eng. C **16**, 27–30 (2001).
[6] R. J. Parmee, C. M. Collins, W. I. Milne, and M. T. Cole, Nano Convergence **2**, 1 (2015).
[7] W. I. Milne, K. B. K. Teo, G. A. J. Amaratunga, P. Legagneux, L. Gangloff, J. P. Schnell, V. Semet, V. T. Binh, and O. Groening, J. Mater. Chem. **14**, 933–943 (2004).
[8] M. Khaneja, L. Bisen, S. Gautam, P. Kumar, J. S. B. S. Rawat, S. Ghosh, P. K. Choudhary, and V. Kumar, Indian J. Pure & Appl. Phys. **51**, 583–586 (2013).
[9] S. H. Jo, J. Y. Huang, S. Chen, G. Y. Xiong, D. Z. Wang, and Z. F. Rena, J. Vac. Sci. Technol. B **23**, 2363–2368 (2005).
[10] L. Cui, J. Chen, B. Yang, and T. Jiao, Nanoscale Res Lett. **10**, 483 (2015).
[11] H. Kimura, B. Zhao, D. N. Futaba, T. Yamada, H. Kurachi, S. Uemura, and K. Hata, APL Mater. **1**, 032101 (2013).
[12] E. Van Hooijdonk, C. Bittencourt, R. Snyders, and J. F. Colomer, Beilstein Int. J. Nanotechnol. **4**, 129–152 (2013).
[13] M. S. Dresselhaus and P. C. Eklund, Adv. Phys. **49**, 705–814 (2000).

[14] K. N. Kudin, B. Ozbas, H. C. Schniepp, R. K. Prud'homme, I. A. Aksay, and R. Car, Nano Lett. **8**, 36–41 (2008).
[15] J. W. Gadzuk and E. W. Plummer, Rev. Mod. Phys. **45**, 487 (1973).
[16] J. M. Bonard, K. A. Dean, B. F. Coll, and C. Klinke, Phys. Rev. Lett. **89**, 197602 (2002).
[17] Z. Xu, X. D. Bai, E. G. Wanga, and Z. L. Wang, Appl. Phys. Lett. **87**, 163106 (2005); R. T. Khare, R. V. Gelamo, M. A. More, D. J. Late, and C. S. Rout, Appl. Phy. Lett. **107**, 123503 (2015).
[18] Z. L. Wanga, R. P. Gao, W. A. de Heer, and P. Poncharal, Appl Phys. Lett. **80**, 856–858 (2002).
[19] A. G. Rinzler, J. H. Hafner, P. Nikolaev, P. Nordlander, D. T. Colbert, R. E. Smalley, L. Lou, S. G. Kim, and D. Tománek, Science **269**, 1550–1553 (1995).
[20] H. Zanin, P. W. May, M. H. M. O. Hamanaka, and E. J. Corat, ACS Appl. Mater. Interfaces **5**, 12238−12243 (2013).
[21] S. Parveen, S. Husain, A. Kumar, J. Ali, Harsh, and M. Husain, J. Exp. Nanosci. **10**, 499–510 (2015).
[22] S. Sridhar, L. Ge, C. S. Tiwary, A. C. Hart, S. Ozden, K. Kalaga, S. Lei, S. V. Sridhar, R. K. Sinha, H. Harsh, K. Kordas, P. M. Ajayan, and R. Vajtai, ACS Appl. Mater. Interfaces **6**, 1986–1991 (2014).
[23] P. H. Lin, L. Sie, C. A. Chen, H. C. Chang, Y. T. Shih, H. Y. Chang, W. J. Su, and K. Y. Lee, Nanoscale Res Lett. **10**, 297 (2015).
[24] B. K. Gupta, G. Kedawat, P. Kumar, S. Singh, S. R. Suryawanshi, N. Agrawal (Garg), G. Gupta, A. R. Kim, R. K. Gupta, M. A. More, D. J. Late, and M. G. Hahm, RSC Adv. **6**, 9932–9939 (2016).
[25] J. Ali, A. Kumar, S. Husain, S. Parveen, R. Choithrani, M. Zulfequar, Harsh, and M. Husain, J. Nanoscience **2014**, 437895.